De novo design and molecular assembly of a transmembrane diporphyrin-binding protein complex

Ivan V. Korendovych,[†] Alessandro Senes,[†,§] Yong Ho Kim,[†] James D. Lear,[†] H. Christopher Fry,[‡] Michael J. Therien,[#] J. Kent Blasie,[‡] F. Ann Walker,[||] William F. DeGrado[†,‡]*

[†]Department of Biochemistry and Biophysics, University of Pennsylvania, [§]Present address: Department of Biochemistry, University of Wisconsin-Madison (A.S. is a primary computational author of this paper), [#]Department of Chemistry, Duke University, [||]Department of Chemistry and Biochemistry, University of Arizona, [‡]Department of Chemistry, University of Pennsylvania.

SUPPORTING INFORMATION

General. Iron(III) diphenylporphyrin (Scheme S1) was prepared using the literature procedure.[S1]

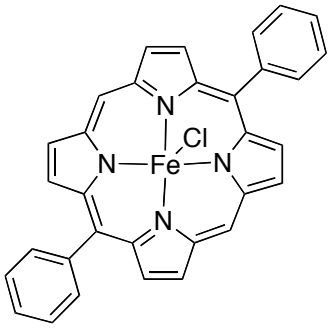

Scheme S1. Chemical structure of Fe^{III}DPP.

Computational design. An idealized D_2 symmetrical coiled coil backbone was generated from parameters as described by North et al.[S2] Minor helix parameters: radius (r_1), 2.23Å; frequency (ω_1), 102.86º; rise per residue (h), 1.51Å; phase (ψ_1), -66.49º. Super helix parameters: radius (r_0), 8.41 Å; pitch (P), 179.30Å; phase (ψ_0), 31.01º; translation along superhelical axis (z_{trans}), 0.01 Å. The parameters were obtained by fitting the model of the four porphyrin binding soluble design 4PA after 4 ps of molecular dynamics.[S3] The section of the backbone corresponding to residues 16-39 in 4PA was selected for the membrane design. This section contains two porphyrin molecules in near contact and a 24 residue size provides a bundle dimension (33 Å) comparable with the hydrophobic thickness of the membrane. In the new construct, the coordinating His residue is position

8 and the Thr residue that provides a second shell hydrogen bond to the His is position 18. Side chains and ligand were placed in two phases, using conformations from a highly dense conformer library for protein design.[S4] In the first phase, the conformation of the keystone resiudes (His8, Thr18 and the porphyrin ligands) was optimized. Fifty His conformers (neutral, δ-protonated) near [$\chi_1 = 180^\circ$, $\chi_2 = 60^\circ$] and 25 Thr conformers near [$\chi_1 = 60^\circ$] were selected from the library. The orientation of the diphenyl-porphyrin ligand was varied according to the His conformer, by placing the Fe atom on the projection of the His Nε2 onto the super-helical axis, and by rotating the plane around the super-helical axis according to the superhelical periodicity of an angle a

$$a = ||z - z_0|| / P * 360$$

where z is the coordinate of the Fe atom, z_0 the center of the bundle and P is the super-helical pitch.

The optimization was performed by exhaustive search and the result with most idealized coordination of geometry and second shell hydrogen bond was chosen among the energetically favorable solutions.

The model has a Nε2 - Fe distance of 2.30 Å, and dihedral angle between the His planes of 82.5º and an angle between porphyrin and His ring planes of 88º. The design was completed with all side chains using Dead End Elimination followed by Monte Carlo/Self Consistent Mean Field to explore the reduced search space. Energies were calculated using the CHARMM22 force field, using the following terms: vdW (with unscaled radii), Coulomb, bond, angle, dihedral, improper and IMM solvation. Positions were divided in 4 categories, those completely buried, mostly buried, mostly exposed, and completely exposed. These were given different degrees of side chain conformational sampling (from most to none, respectively). The conformations were selected from the conformer library using a procedure that involved constrained minimization of the side chain against the backbone (with all variable positions mutated to Gly) and selection of the desired number of conformers after exclusion of those with steric clashes. The results were ranked as binding energies as

$$E_{\text{binding}} = E_{\text{b}} - E_{\text{u}}$$

where E_{b} is the energy of the complex, and E_{u} is the energy after the helices have been separated at 2000 Å and the side chain relaxed using MC/SCMF. The lowest energy

sequence is Ac-**AIYGI LAHSL ASILA LLTGF LTIW**-$CONH_2$, nicknamed PRIME. It is compared with the appropriate region of 4PA below:

AIYGILAHSL ASILALLTGF LTIW
AQQALQEHRQ ALQAAQQTAQ KAQQ

The key residues (His, Thr) are shown in red. Identical and similar residues are shown in blue and green, respectively. As you can see the major difference is in the residues facing the outside but the cores are very similar.

Peptide Synthesis. Peptides were synthesized using a Symphony peptide synthesizer (Protein Technologies, Inc.) at 0.1 mmol scales using a Fmoc-PAL-PEG -PS resin (Applied Biosystems) with a substitution level of 0.21 mmol/g. Activation of the free amino acids (5 fold excess) was achieved with 0.95 equiv (relative to the amino acid) excess of HATU in the presence of 10 equiv of DIEA. The reaction solvent contains 25% DMSO and 75% NMP (HPLC grade, Aldrich). Side chain deprotection and simultaneous cleavage from the resin was performed using a mixture of TFA/triethylsilane/water (95:2.5:2.5 v/v) at room temperature, for 3 hours. After filtration most of the solvent was evaporated using a stream of N_2. The crude peptides collected from precipitation with cold diethyl ether (Aldrich) were dried in vacuo. The peptides were then purified on a preparative reverse phase HPLC system (Varian ProStar 210) with a C4 preparative column (Vydac) using a linear gradient of buffer A (0.1% TFA in Millipore water) and buffer B' (6:3:1 2- propanol:acetonitrile:water) containing 0.1% TFA. Elution of the purified peptides occurred at approximately 77% of buffer B'. The identities of the purified peptides were confirmed by MALDI-TOF mass spectroscopy on a Voyager Biospectrometry Workstation (PerSeptive Biosystems), and their purity was assessed using HP1100 analytical HPLC system (Hewlett Packard) with an analytical C4 column (Vydac) and a linear A/B' gradient.

Analytical Ultracentrifugation. Equilibrium sedimentation was used primarily to determine the association state of the peptides, and also to provide an estimate of the association constants. The experiments were performed in a Beckman XL-I analytical ultracentrifuge (Beckman Coulter) using six-channel carbon-epoxy composite

centerpieces at 25 °C. Peptides were co-dissolved in CF_3CH_2OH (Sigma) and DPC (dodecyl phosphatidylcholine, Avanti Polar Lipids). The organic solvent was removed under reduced pressure to generate a thin film of peptide/detergent mixture, which was then dissolved in buffer previously determined to match the density of the detergent component (10 mM phosphate buffer (pH= 7.4) buffer containing 52% D_2O). The final concentration of DPC is 15 mM in all of the samples. Samples were prepared in a total peptide concentration of 50 μM for apo PRIME, for 16 μM holo PRIME and 120 μM for holo PRIME Q-band measurements. The holo samples included 0.5 equiv of iron(III) diphenylporphyrin chloride. Data at different measurement speeds (40, 45 and 50 krpm for apo PRIME; 35, 40, 45 and 50 krpm for holo PRIME; and 30, 35, 40, 45, and 50 krpm for holo PRIME at Q-band) were analyzed by global curve-fitting of radial concentration gradients (measured using optical absorption) to the sedimentation equilibrium equation for monomer-tetramer equilibria among the peptides included in the solution. Peptide partial specific volumes were calculated using previously described methods[5] and residue molecular weights corrected for the 52% D_2O exchange expected for the density-matched buffer. The solvent density (1.059 g/ml) was measured using a Paar densitometer. Aqueous solution molar extinction coefficients at 280 nm were calculated using the program Sednterp.[S6] These coefficients were multiplied by the molar detergratio concentration units.

Sedimentation equilibrium data were fit using Igor Pro (Wavemetrics) to the following equations:

for homotetrameric association of apo PRIME

$$Abs = E + \varepsilon_a c_{0a} l \exp\left[\frac{\omega^2}{2RT} M_a (r^2 - r_0^2)\right] + 4\varepsilon_a \frac{c_{0a}^4}{K_a} l \exp\left[\frac{\omega^2}{2RT} 4M_a (r^2 - r_0^2)\right] \qquad \textbf{(S1)}$$

where E = baseline (zero concentration) absorbance, c_{oa} is the molar PRIME/detergent ratio at r_o; ε_a is the molar extinction coefficient of PRIME at 280 nm, l is the optical path length, $\omega = 2\pi * RPM$, $R = 8.3144 \times 10^7$ erg $K^{-1}mol^{-1}$, T is temperature in K, M_a is the buoyant molecular weight of monomeric PRIME; K_a is the homotetrameric dissociation constant for PRIME.

for holo PRIME at the high peptide/detergent molar ratio, the sedimentation equilibrium was fitted to a single species model:

$$Abs = E + \varepsilon_{assembly} c_{0assembly} l \exp\left[\frac{\omega^2}{2RT} M_{assembly}(r^2 - r_0^2)\right] \quad \textbf{(S2)}$$

where E = baseline (zero concentration) absorbance, $c_{oassembly}$ is the assembly/detergent ratio of PRIME-Fe^{III}DPP at r_o, $\varepsilon_{assembly}$ is the molar extinction coefficient (Q band) of PRIME-Fe^{III}DPP, l is the optical path length, $\omega = 2\pi$*RPM, R= 8.3144 $\times 10^7$ erg K^{-1}mol^{-1} , T is temperature in K, M_{assembly} is the buoyant molecular weight of PRIME-Fe^{III}DPP complex.

In the absence of the cofactor PRIME is more than 90% monomeric. Also Fe^{III}DPP is not soluble in DPC micelles under the typical AUC experimental conditions, thus the dissolved cofactor is associated with PRIME. Therefore we have used the following model to describe the association of PRIME with the cofactor at lower PRIME/detergent molar ratios:

$$2\ \text{PRIME*Cofactor} + 2\ \text{PRIME} \rightleftharpoons \text{PRIME}_4\text{*Cofactor}_2$$

$$Abs = E + \frac{1}{2}\varepsilon_{assembly} c_{0ab} l \exp\left[\frac{\omega^2}{2RT}(M_a + M_b)(r^2 - r_0^2)\right] + \varepsilon_{assembly} \frac{c_{0ab}^2 c_{0a}^2}{K_{ab}} l \exp\left[\frac{\omega^2}{2RT}(4M_a + 2M_b)(r^2 - r_0^2)\right] \quad \textbf{(S2)}$$

where E = baseline absorbance, c_{oa} and c_{oab} are the molar concentrations of PRIME and PRIME-cofactor (1:1) complex, respectively, at r_o, $\varepsilon_{assembly}$ is the molar extinction coefficient of the Soret band (at 409 nm) in the PRIME-Fe^{III}DPP (4:2) complex, l is the optical path length, $\omega = 2\pi$*RPM, R= 8.3144 $\times 10^7$ erg K^{-1}mol^{-1} , T is temperature in K, M_a *and* M_b are the buoyant molecular weights of monomeric PRIME and the cofactor, respectively; K_{ab} is the heteromeric dissociation constant for a complex comprising 4 PRIME monomers and 2 molecules of the cofactor.

Molecular weight was obtained from the buoyant molecular weight using:

$$M_w = M(1 - \bar{v}\rho) \quad \textbf{(S4)}$$

where M is the buoyant molecular weight, $\bar{v}$ is the partial specific volume and ρ is the solution density.

Circular Dichroism Spectrometry. CD spectrometry experiments were carried out using a J- 810 spectropolarimeter (JASCO). Peptide samples were prepared at 50 μM concentration in micelles (2 mM dodecyl phosphatidylcholine, Sigma) with and without the cofactor (25 μM) in 10 mM phosphate buffer pH = 7.4 in a 1 mm pathlength quartz cell for the measurements between 190 and 260 nm. A sample containing 15 μM peptide and 7.5 μM Fe(III) diphenylporphyrin chloride in a 1 cm was used to collect a CD spectrum in the Soret band region (360-460 nm). Measurements were conducted at 20°C in step scanning mode with a response time of 4 seconds. Three independent measurements were collected and averaged.

EPR studies. Unless explicitly noted, EPR samples were prepared at 3.1 mM peptide concentration with 1.5 mM Fe^{III}DPP in 185 mM DPC micelles in aqueous buffer containing 30% glycerol. The samples were frozen slowly in liquid nitrogen to avoid sample tube breakage. Spectra were recorded at 4.2 K on a Bruker ESP-300E EPR spectrometer operating at X-band, using 0.2 mW microwave power, 100 kHz modulation frequency, and 2-4 G modulation amplitude. A Systron-Donner frequency counter was used to measure the microwave frequency for precise calculation of g-values. The high-spin Fe(III) porphyrin does not represent a substantial amount of total iron in the sample, moreover samples run at a substochiometric ratio show essentially no high-spin Fe(III) porphyrin present (compare Figures S9 and S10, Supporting Information).

Sample preparations for peptide titrations. Titration samples were prepared in two different ways. The slow equilibration method refers to mixing pre-made stocks of peptide and cofactor in detergent micelles and letting them equilibrate slowly, whereas fast equilibration method refers to making individual samples by mixing the peptide stock with the cofactor in organic solvent followed by reconstitution in buffer. Full

equilibration is achieved in less than 12 hours using the fast equilibration method.The fast equilibration method takes advantage of efficient pre-mixing of components prior to reconstitution in buffer, however its precision suffers from the fact that all titration points are in fact independent experiments. The slow equilibration method employs stock solutions of peptide and cofactor in DPC micelles and is therefore inherently more precise, however full equilibration requires much more time. Titration curves obtained by these two methods agree very well (Figure 2 in the main text).

Potentiometric titrations. Redox titration were done in an anaerobic optical glass cuvette using a platinum electrode and a reference saturated calomel electrode (SCE) using a literature procedure.[S7] Reported potentials are referred to the Normal Hydrogen Electrode using 0.2444 V as the conversion factor. The data were fit to the following equation:

$$X_{red} = \frac{Abs(420nm) - Abs_{\min}(420nm)}{Abs_{\max}(420nm) - Abs_{\min}(420nm)} = \frac{0.5}{1+\exp\left(\frac{n_1(E-E_1)}{25.2}\right)} + \frac{0.5}{1+\exp\left(\frac{n_2(E-E_2)}{25.2}\right)} \quad \textbf{(S5)}$$

where E (mV) is solution potential; E_1 and E_2 (mV) are the redox potentials for the $Fe^{III}Fe^{III}/Fe^{II}Fe^{III}$ and the $Fe^{III}Fe^{II}/Fe^{II}Fe^{II}$ redox couples, respectively; X_{red} is fraction reduced; Abs(420nm) is sample absorbance at 420 nm at a given potential; Abs_{max}(420nm) and Abs_{min}(420nm) are maximum and minimal absorbances at 420 nm, respectively.

In the fits n_1 and n_2 were fixed at 1. If allowed to fit independently, these parameters converge to values near 1.

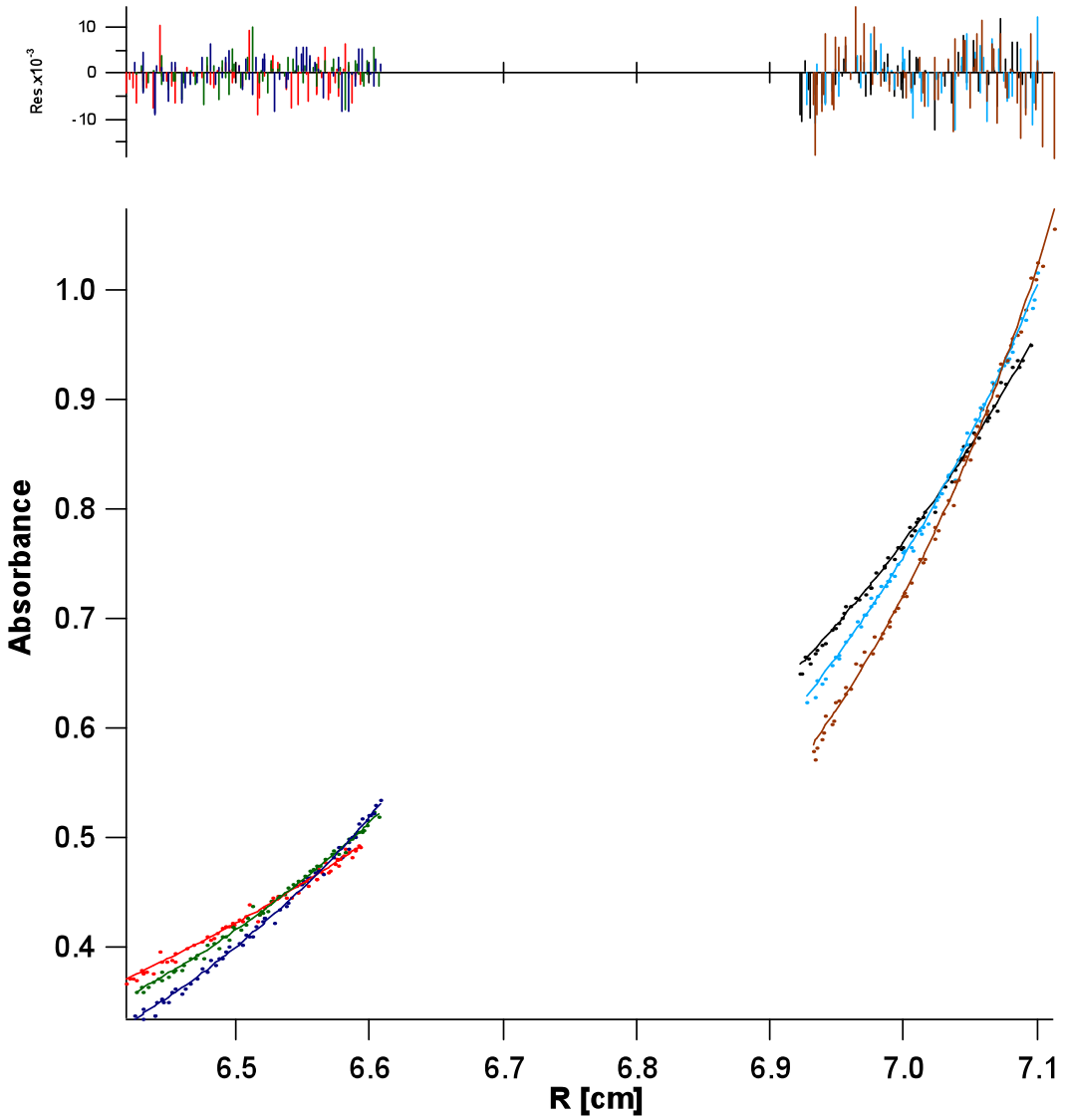

Figure S1. Sedimentation equilibrium profile at 280 nm of PRIME peptide (50 μM) in the absence of the cofactor in density matched DPC micelles (15 mM) in phosphate buffer (10 mM, pH 7.4). The partial specific volume and the solution density were fixed at 0.78524 mL/g and 1.059 g/mL. The data was analyzed using a global fitting routine. The molecular weight was held at 2619.7 and the data were fit to tetramer-monomer $K_d = 1.8\times10^{-5}$ ([peptide]/[detergent])^3 corresponding to the half-dissociated molar ratio of 0.041 ([peptide]/[detergent]).

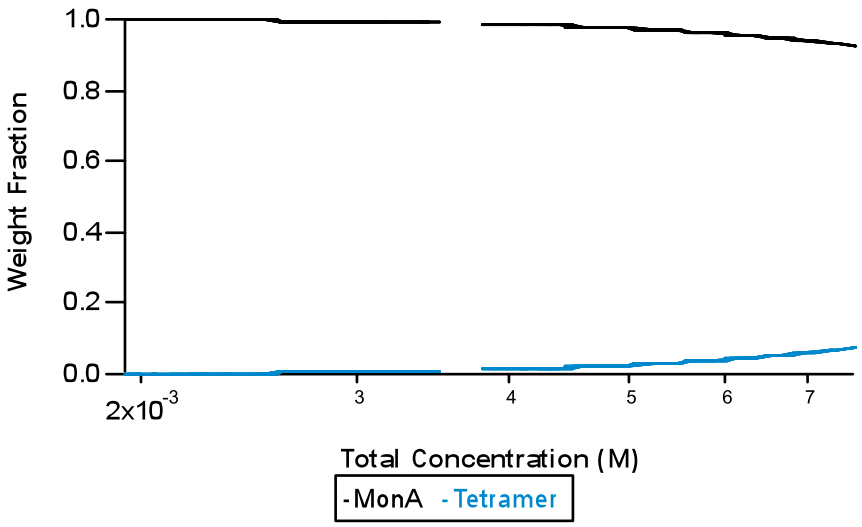

Figure S2. Species distribution plot for sedimentation analysis of PRIME in the absence of the cofactor.

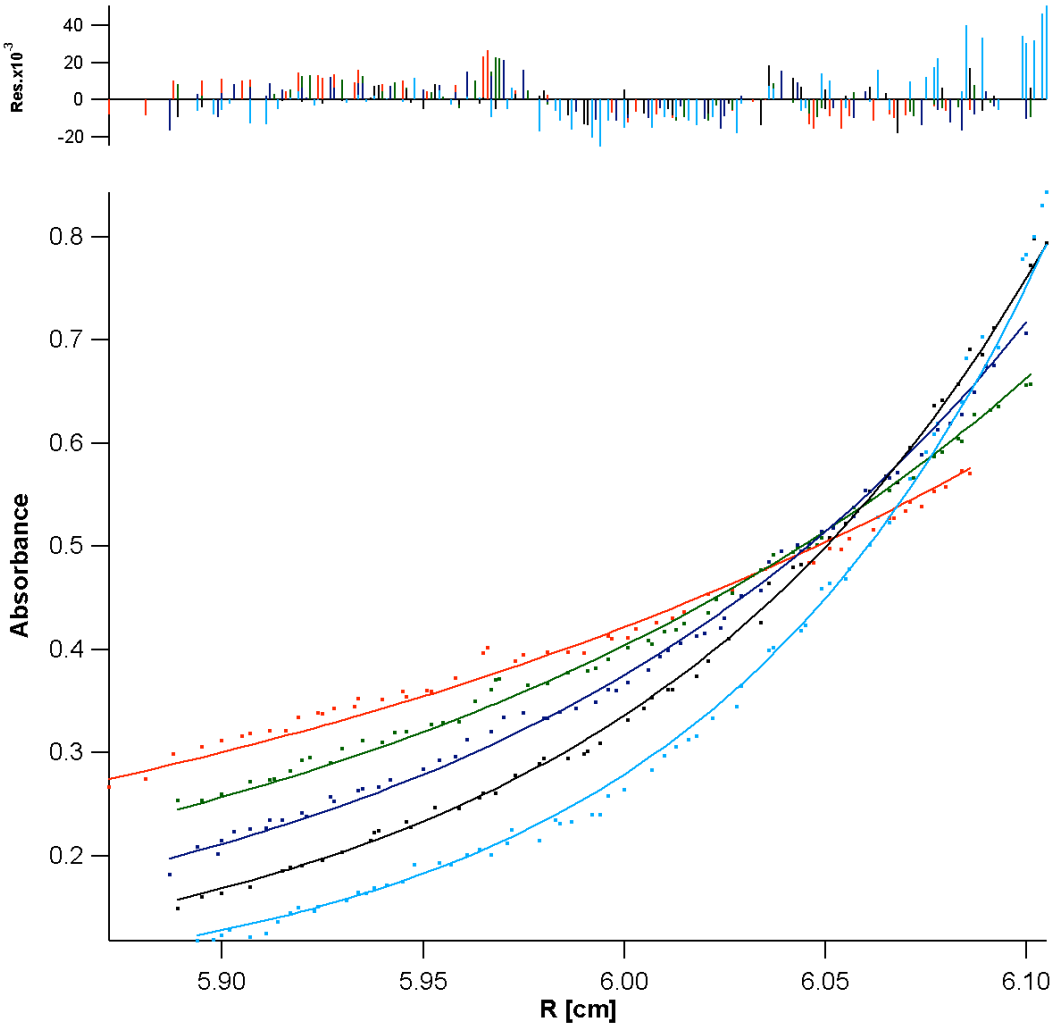

Figure S3. Sedimentation equilibrium profile at 537 nm of PRIME peptide (120 μM) in the presence of 0.5 equiv of cofactor in density matched DPC micelles (15 mM) in phosphate buffer (10 mM, pH 7.4). The partial specific volume and the solution density were fixed at 0.79191 mL/g and 1.059 g/mL, respectively. The data was analyzed using a global fitting routine. The average molecular weight obtained from the fit (10462 Da) corresponds well to the theoretically predicted assembly weight of 11511 Da.

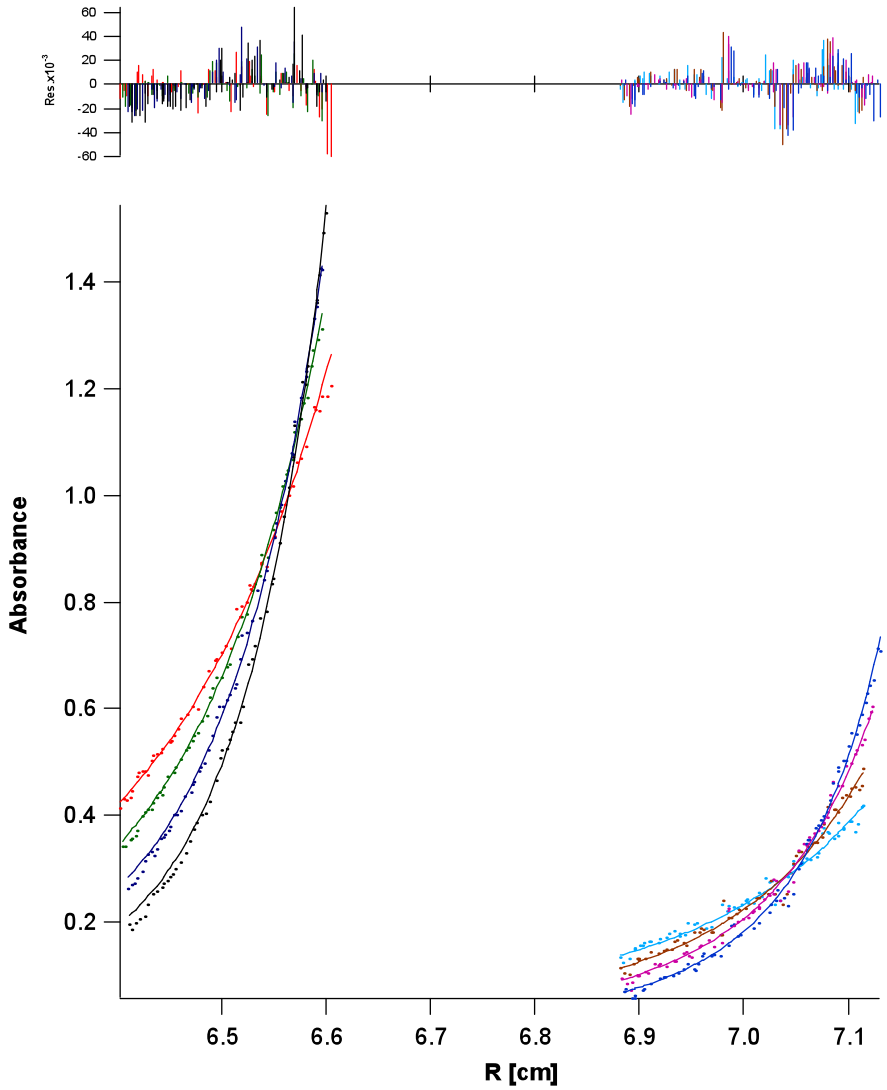

Figure S4. Sedimentation equilibrium profile at 409 nm of PRIME peptide (16 μM) in the presence of 0.5 equiv of cofactor in density matched DPC micelles (15 mM) in phosphate buffer (10 mM, pH 7.4). The partial specific volume and the solution density were fixed at 0.79191 mL/g and 1.059 g/mL, respectively. The data was analyzed using a global fitting routine. The data were fit to a tetramer-monomer $K_d = 1.3 \times 10^{-10}$ ([peptide]/[detergent])^3, corresponding to the half-dissociated molar ratio of 8×10^{-4} ([peptide]/[detergent]).

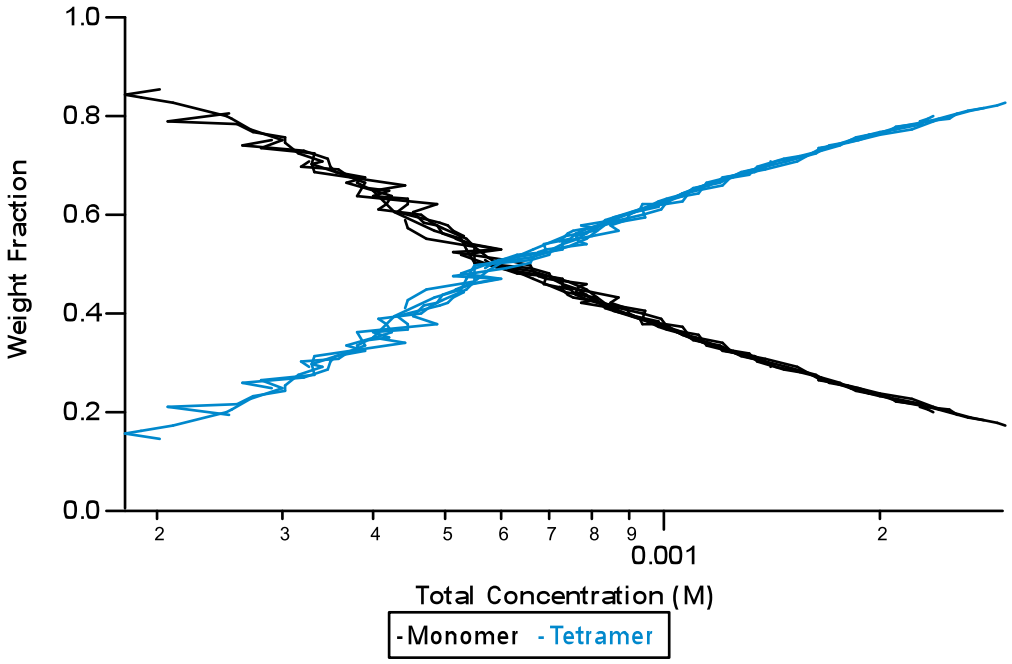

Figure S5. Species distribution plot for sedimentation analysis of PRIME in the presence of 0.5 equiv of iron(III) diphenylporphyrin.

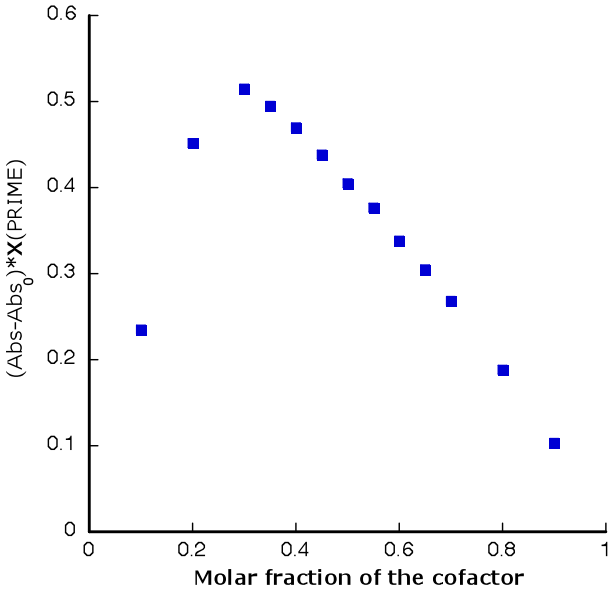

Figure S6. Job's plot of PRIME and Fe(III)DPP-Cl (total concentration of peptide and the cofactor is 24 μM) in DPC micelles (2 mM).

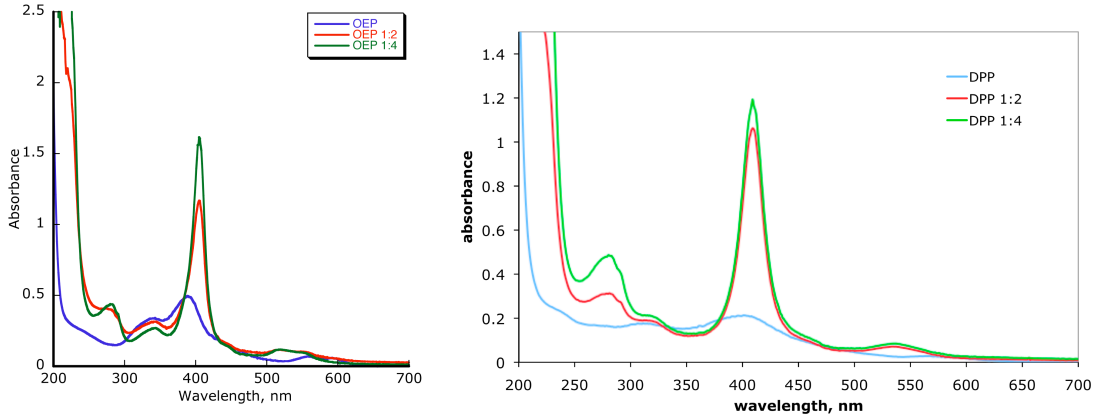

Figure S7. Left: spectra of iron(III) octaethylporphyrin (12 μM) in DPC micelles (3 mM) in phosphate buffer (10 mM, pH 7.4) upon addition of 0 equiv (blue), 2 equiv (red) and 4 equiv (green) of PRIME. Right: the corresponding results for iron(III) diphenylporphyrin done under the same conditions.

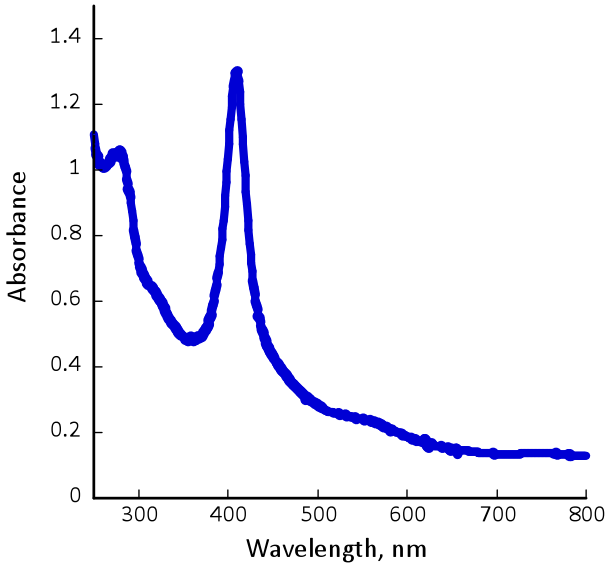

Figure S8. UV-vis spectrum of PRIME assembled in Fe^{III}DPP in POPC lipid bilayers (SUV's), diluted 2 fold. Starting concentrations are: POPC 12.5 mM; PRIME 125 μM; cofactor 62 μM. Buffer conditions TRIS (10 mM), pH 7.4.

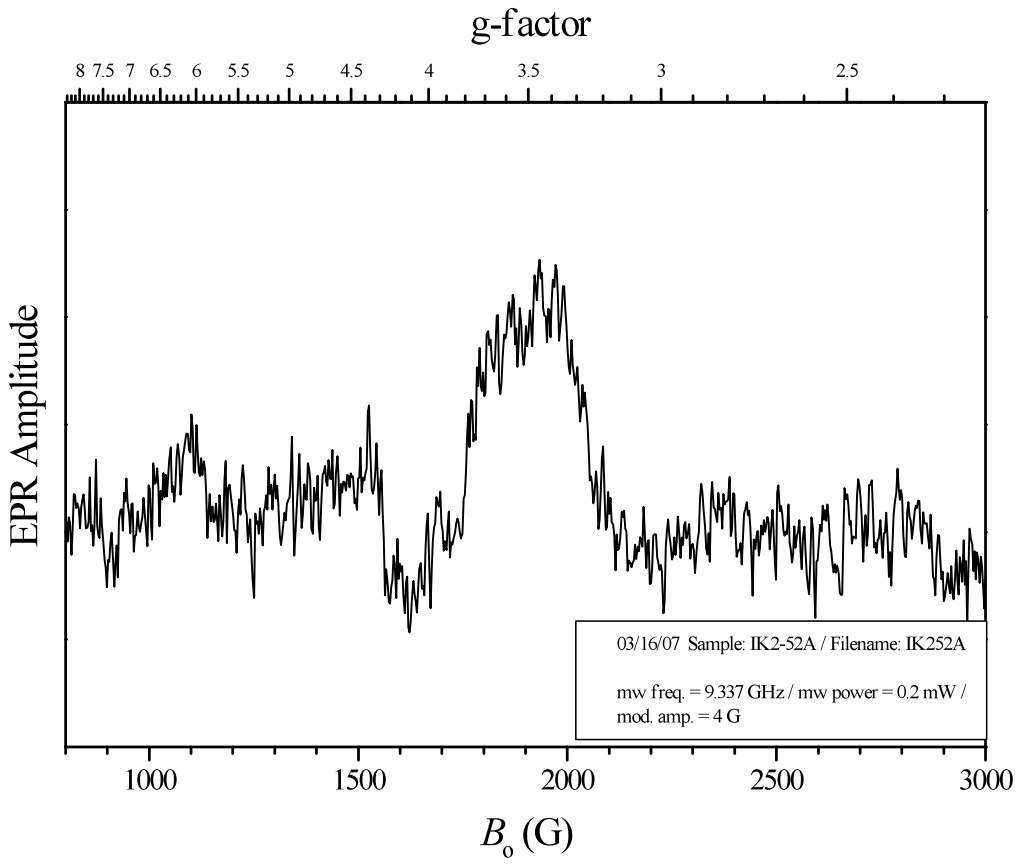

Figure S9. EPR spectrum of PRIME with Fe^{III}DPP in 1:1 cofactor:bundle stoichiometry at 4.2 K showing essentially no high spin iron(III) porphyrin present. The sample contains 0.3 mM Fe^{III}DPP, 1.2 mM peptide, 48 mM of DPC reconstituted in 40 mM phosphate buffer, pH 7.4 with no glycerol added.

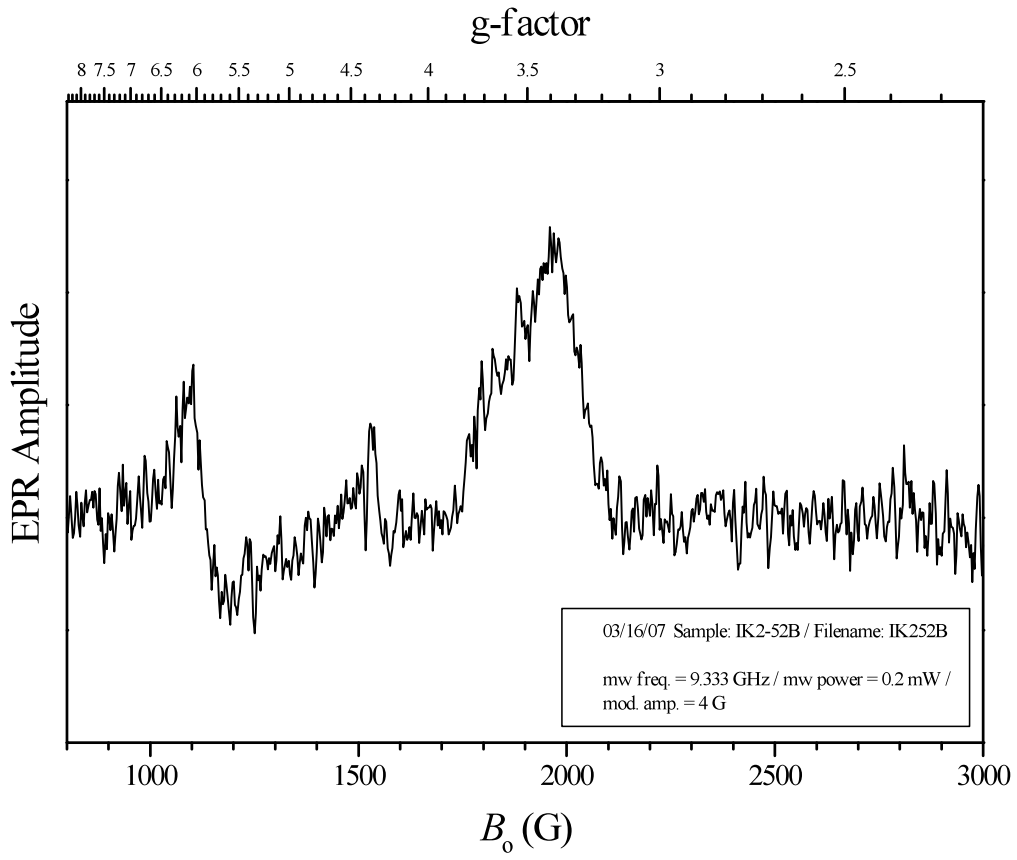

Figure S10. EPR spectrum of PRIME with Fe^{III}DPP in 2:1 cofactor:bundle at 4.2 K. The sample contains 0.4 mM Fe^{III}DPP, 0.8 mM peptide, 32 mM of DPC reconstituted in 40 mM phosphate buffer, pH 7.4 with no glycerol added.

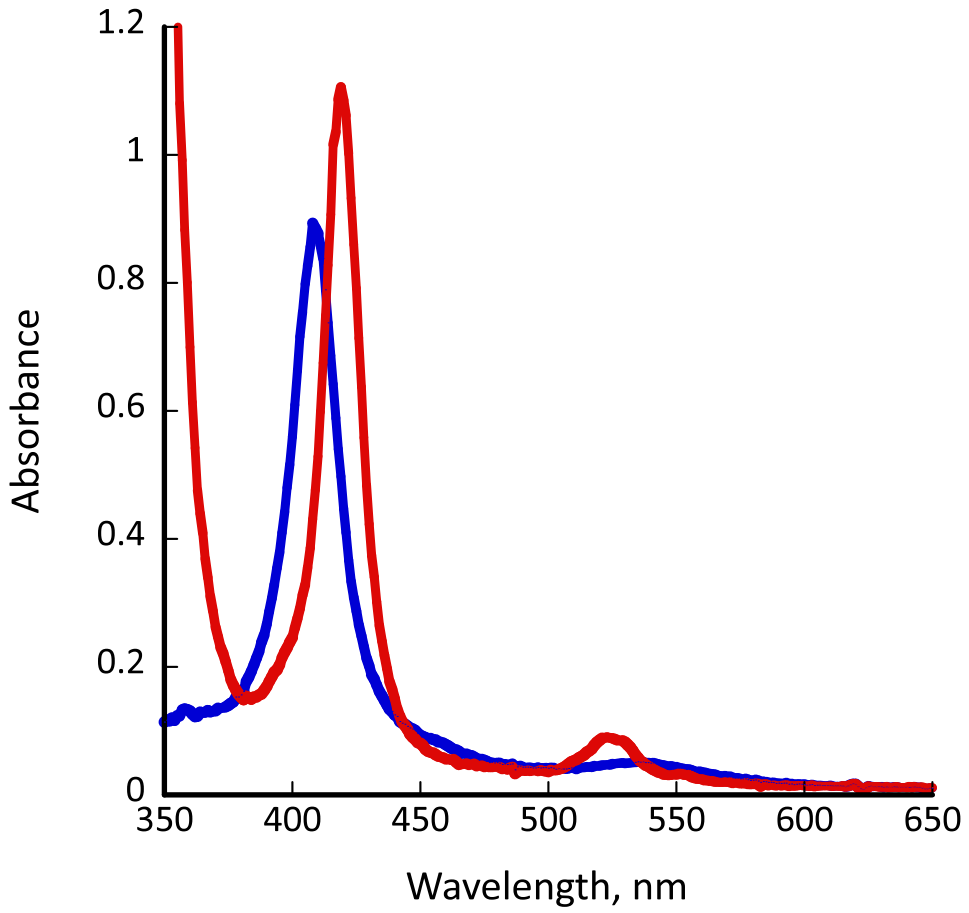

Figure S11. Reduction of PRIME-Fe^{III}DPP (8 μM cofactor, 16 μM peptide) with excess sodium dithionite in DPC micelles (16 mM).

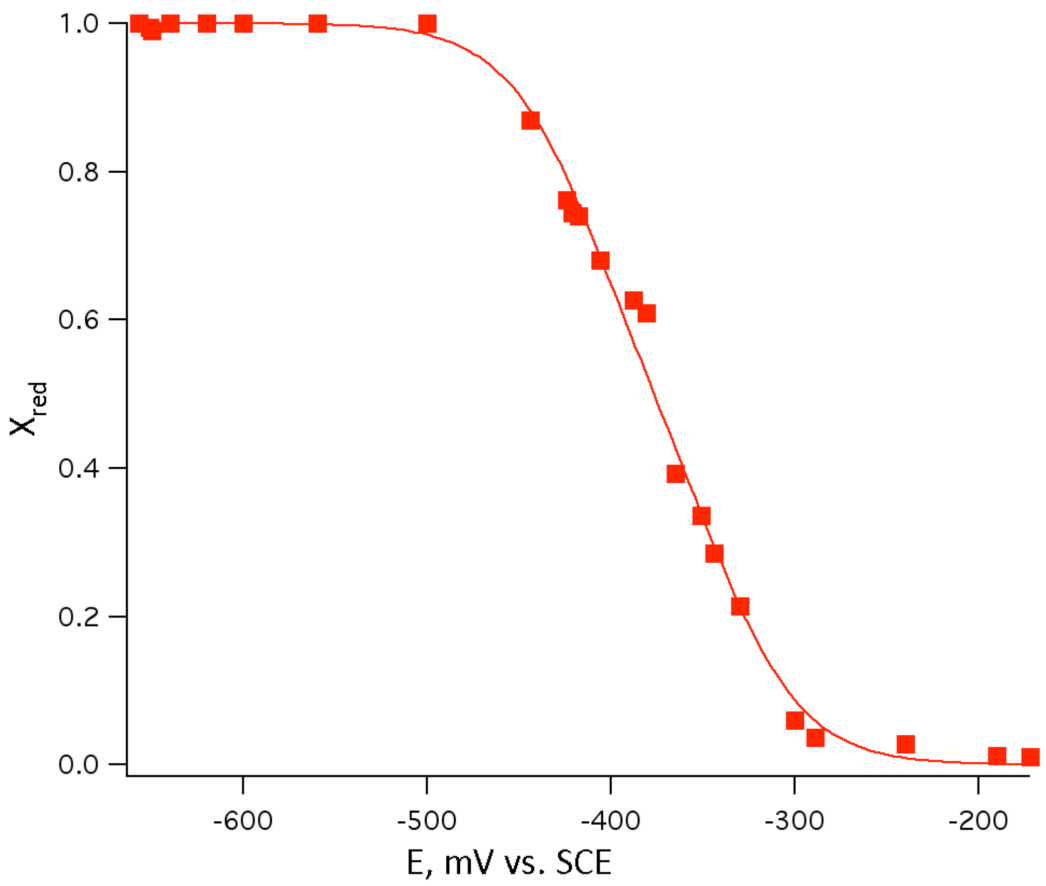

Figure S12. Plot of the fraction reduced of PRIME-Fe(III)DPP assembly vs. solution potential (vs. SCE). The apparent $E_{1/2}(Fe^{III}Fe^{III}/Fe^{II}Fe^{III})$ and $E_{1/2}(Fe^{III}Fe^{II}/Fe^{II}Fe^{II})$ are the -341±3 mV (-97±3 mV vs NHE) and -412±3 mV (-168±3 mV vs NHE).

REFERENCE

(S1) Jaquinod, L.; Prevot, L.; Fischer, J.; Weiss, R. *Inorg. Chem.* **1998**, *37*, 1142-1149.
(S2) North, B.; Summa, C. M.; Ghirlanda, G.; DeGrado, W. F. *J. Mol. Biol.* **2001**, *311*, 1081-1090.
(S3) McAllister, K. A.; Zou, H.; Cochran, F. V.; Bender, G. M.; Senes, A.; Fry, H. C.; Nanda, V.; Keenan, P. A.; Lear, J. D.; Saven, J. G.; Therien, M. J.; Blasie, J. K.; DeGrado, W. F. *J. Am. Chem. Soc.* **2008**, *130*, 11921-11927.
(S4) *The conformer library is available as a separate file as part of the online Supporting Information package.*
(S5) Durchschlag, H.; Zipper, P. *Progr. Colloid and Polym. Sci.* **1994**, *94*, 20-39.
(S6) Lebowitz, J.; Lewis, M. S.; Schuck, P. *Protein Sci.* **2002**, *11*, 2067-2079.
(S7) Discher, B. M.; Noy, D.; Strzalka, J.; Ye, S.; Moser, C. C.; Lear, J. D.; Blasie, J. K.; Dutton, P. L. *Biochemistry* **2005**, *44*, 12329-12343.